Planar-Motion Correction with Use of K-space Data Acquired in Fourier MR Imaging[1]

Michael L. Wood, PhD • Mansur J. Shivji, BSc • Peter L. Stanchev, PhD

The authors have developed a method for reducing magnetic resonance (MR) image artifacts caused by planar motion. Segments of k-space acquired with the subject stationary are detected automatically. Each k-space segment is Fourier transformed into an image in which rotational and translational displacements are measured manually. Before correction, k-space is made as Hermitian as allowed by the largest symmetric range of low spatial frequencies acquired with the subject stationary. Segments of k-space acquired with the subject in different positions are corrected separately. Although translation corrections can be applied effectively to both k-space and the spatial domain, rotation corrections are applied in the spatial domain to avoid image artifacts. To complement the correction, data corrupted by rotation are replaced by the complex conjugate of data of the opposite k_x and k_y, provided that these data have not been corrupted by rotation. The method reduced ghosts and blurring substantially on sagittal head images acquired with a standard spin-echo pulse sequence while a volunteer subject nodded his head.

Index terms: Artifact • Image processing • K-space • Motion correction

JMRI 1995; 5:57–64

Abbreviations: FOV = field of view, RMSE = root-mean-square error, 2D = two-dimensional

MOVEMENT RANGING from rapidly flowing blood to relatively slow body movements, such as nodding of the head or shifting of position, often causes artifacts on magnetic (MR) resonance images (1–4). Body movements are encountered frequently during MR imaging of infants, children, and uncomfortable, disoriented, or otherwise restless patients. Nodding of the head is a particularly interesting movement, because the entire head moves essentially within a plane and possibly only a few times during the acquisition of data for an MR image.

Fourier imaging techniques, which are the most common, produce data that represent the imaged anatomy in k-space (5,6). Usually, the data are samples of k_x and k_y, which are spatial frequencies along the x and y directions. The entire range of k_x values for each k_y value is obtained from one echo, which is sampled rapidly relative to body motion. However, it takes from several seconds to several minutes to acquire all the k_y values, during which considerable motion can occur (7).

Motion modifies the characteristics of k-space. Translation within the plane of a two-dimensional (2D) image alters the phase of the k-space samples (8). Spatial rotation results in a corresponding rotation of k-space (9). These properties have been exploited in various methods to compensate for motion (10–13). We hypothesize that changes to k-space due to body movements can be identified. Segments of k-space acquired during constant position can then be isolated and reconstructed separately into images, from which planar displacements can be measured. These displacement measurements can be used to correct k-space for the effects of motion. In evaluating the above hypotheses, we have developed a method to correct for planar motion. This method is described below and demonstrated by using experimental data acquired while a volunteer nodded his head.

• MATERIALS AND METHODS

A conventional 2D spin-echo pulse sequence on a commercial 1.5-T MR imaging system (GE Medical Systems, Milwaukee, Wis) was used to acquire k-space data for a single-section sagittal MR image through the head of a volunteer subject nodding his head. For reference, k-space data were acquired under the same conditions while the subject remained stationary. The head coil was used with a pillow

[1] From the Department of Medical Imaging, University of Toronto and St Michael's Hospital, 30 Bond St, Toronto, Ontario, Canada M5B 1W8 (M.L.W.); and the Imaging Research Program, Sunnybrook Health Science Centre, Toronto, Ontario, Canada (M.J.S., P.L.S.). Received February 10, 1994; revision requested March 30; revision received and accepted June 14. Supported in part by Medical Research Council of Canada grant MT-11574 and Sterling-Winthrop Imaging Research Institute grant RP2021. **Address reprint requests to** M.L.W.

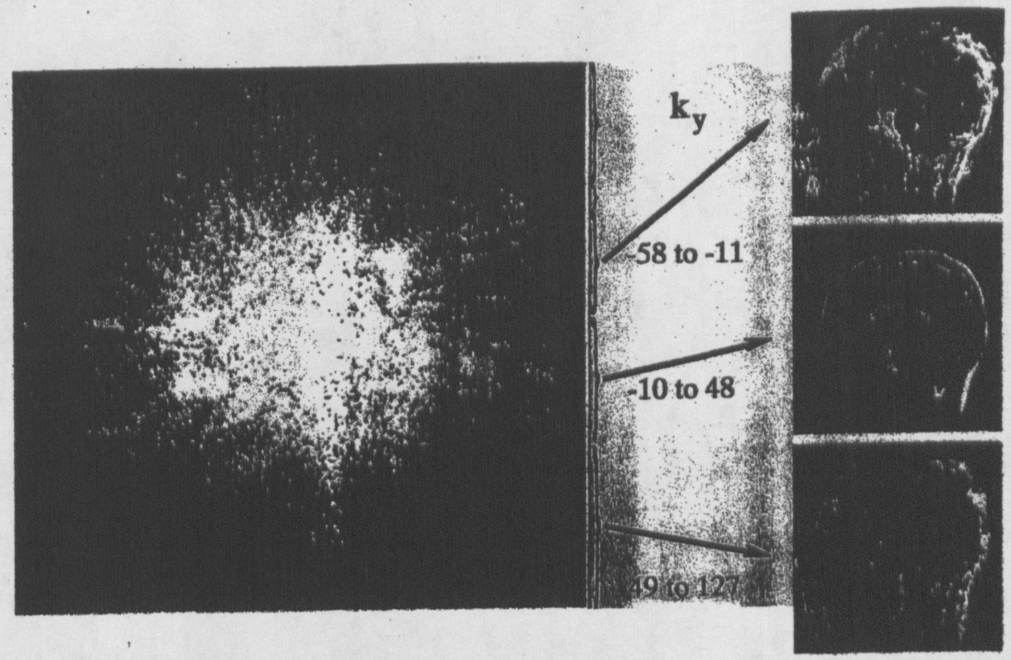

Figure 1. Subject motion seen on images from segments of k-space. Each k-space row, which is identified by a different k_y value, was filled with consecutive echoes from a conventional spin-echo pulse sequence. Discontinuities between rows of k-space suggest that the subject moved five times during data acquisition. Images from three of the five k-space segments between these discontinuities show head movement in the sagittal plane. The modulus of the complex numbers in k-space and the images are displayed. All images were scaled to the same maximum intensity.

placed inside it to help keep displacements within the sagittal plane. Relevant imaging parameters included TR msec/TE msec = 500/16, two signals acquired, 5-mm section thickness, and 300-mm field of view (FOV). The k-space composed of k_x and k_y ranging from −128 to 127 cycles per FOV was filled linearly from the extreme negative k_y to the extreme positive k_y.

The k-space data were analyzed on a computer workstation to identify k_y values acquired during subject movement, and hence segments acquired when the subject's position remained constant. Movement was found to cause abrupt changes along the k_y direction. These changes were detected automatically by means of a paired *t* test comparing the complex k-space samples for each k_y and the corresponding samples for the previous k_y. Alternatives such as edge detectors derived from forward or backward differences were explored first, but they were discarded after the paired *t* test proved to be more effective. Movements were expected to make the *t* test *P* value small for at least two consecutive k_y values. The subject's position was suspected to have changed at a particular k_y if the *P* values for both that k_y and the next k_y were below a threshold, which was chosen to be .01 after experimentation.

The segment of k-space between abrupt changes along k_y was isolated and then reconstructed into an image, as follows. First, the segment was copied to a blank array the same size as k-space. This partial k-space was made Hermitian by copying the complex conjugate of each sample in the segment to the location indexed by k_x and k_y of opposite sign (14). Hermitian symmetrization was necessary to avoid the blurring associated with Fourier transformation of a distribution truncated asymmetrically with respect to the center of k-space (15,16). A 2D inverse Fourier transform of the symmetrized partial k-space, followed by the modulus operator, yielded the desired image. The images were analyzed manually to determine the displacement that had occurred during data acquisition. The image corresponding to the central k-space segment was designated as the reference, although any segment could have been chosen. Images from the other segments were rotated and translated to achieve registration with a contour derived from the reference image.

An experiment was designed to assess the accuracy of displacement measurements in images reconstructed from a k-space having nonzero samples for only a few k_y values. Segments of various size and centered on different k_y were isolated from the k-space data acquired with the head stationary. Images from each segment were reconstructed as already described and then rotated and translated by amounts up to 30° and 20 pixels in the x and y directions. Without knowledge of these displacements, three individuals measured the displacements relative to a reference image. The error between the measured and known displacements was computed.

Theoretically, corrections for planar translation or rotation could be applied to either k-space or the spatial domain (10). The effects of translation were corrected by means of a linear phase shift in k-space (8). The k-space domain was preferred for translation corrections because of the ease of compensating for fractional-pixel displacements. Rotations in space are known to cause an equivalent rotation in k-space (9,10). The following experiment evaluated the effects of rotation applied in either k-space or the spatial domain and the method for interpolating to achieve rotation, specifically 2D nearest-neighbor, linear, and cubic-spline interpolation. Each proposed rotation was applied to the entire k-space or image twice, first 45°, then −45°, so that the net rotation was zero. Artifacts and other errors were identified visually and by calculating the root-mean-square error (RMSE) between the complex numbers in the rotated image or k-space and the unmodified image or k-space. The RMSE for the images was expressed as a percentage of the mean intensity in a region within the midbrain on the reference image. The k-space RMSE was expressed as a percentage of the mean modulus of the entire reference k-space.

Artifacts were expected if different spatial transformations were applied to k-space segments, unless

Table 1
Rotation and Translation Measurements in Images from K-Space Segments

K-space Segment		x-Translation	y Translation	
Rows	k_y	Rotation	(pixels)	(pixels)
1–57	−128 to −72	2°	−14	−3
58–70	−71 to −59	−17°	−17	−1
71–118	−58 to −11	−17°	−18	−2
119–177	−10 to 48	0°	0	0
178–256	−49 to 127	−6°	−20	−3

the image from each segment was purely real, which would be true for a Hermitian k-space (14). As an experiment, data acquired with the head stationary were made Hermitian through a global phase correction based on the entire k-space (15,16). Namely, k-space was subjected to a 2D inverse Fourier transform, and the complex numbers associated with each pixel were made real by using a high-resolution phase image derived from the entire k-space. This real image was rotated 45° by using nearest-neighbor interpolation and then Fourier transformed back to k-space. A reference k-space was synthesized from the first 126 rows of the rotated k-space (−128 cycles per FOV ≤ k_y ≤ −3 cycles per FOV) and the last 130 rows of the nonrotated k-space (−2 cycles per FOV ≤ k_y ≤ 127 cycles per FOV). For testing, a non-Hermitian k-space was constructed by shifting each row of the reference k-space by five columns. A rotation correction was applied in the spatial domain to reverse the 45° rotation affecting the first 126 rows of both the reference and test k-spaces. This correction left the reference k-space Hermitian but not the test k-space. One-dimensional and 2D inverse Fourier transforms of each k-space were compared.

The sensitivity of proposed corrections to displacement-measurement errors was studied by applying an erroneous displacement correction to segments of k-space associated with the stationary head. Instead of no displacement, an angular displacement of 2.0° and a translation of 2.0 pixels in the x and y directions were assumed to have occurred. Each segment spanned nine k_y values, with the central k_y values ranging from eight to 96 cycles per FOV. A complex image reconstructed from the supposedly corrected k-space was subtracted from a complex image reconstructed from the unmodified k-space. The RMSE in this difference image was computed as a measure of the error resulting from an erroneous displacement measurement.

The planar-motion correction method was tested on the k-space obtained while the subject's head was moving. This experiment involved correcting for different displacements in multiple k-space segments. Each segment was processed separately, and the results were accumulated in an array that became the corrected k-space. Rotation moved data into different rows and columns. When rotation caused data to overlap, data originating from the closest k-space coordinates were retained. Alternatives such as retaining the largest overlapping data sample and summing or averaging the overlapping data were considered but not incorporated into the method. Different corrections for data in the first and last rows of each segment were explored but also not incorporated.

As a refinement to compensate for imperfections attributed to the rotation correction, data corrupted by rotation were replaced by data corresponding to k_x and k_y of opposite sign, provided the latter were unaffected by rotation. Finally, data that were not intended to be corrected were copied to the corrected k-space array last, so that they would overwrite any data that became located on k_x and k_y values that had not been corrupted by motion.

• RESULTS

Several rows of the k-space acquired while the subject nodded his headed appeared anomalous (Fig 1). The paired *t* test with a *P*-value threshold of .01 identified these anomalous rows, which are listed in Table 1. The same test with .1 as the threshold added row 130 to the list. However, analysis of the image reconstructed from k-space data near row 130 found no evidence of displacement. The *P* value for every row listed in Table 1 was less than .0001. The threshold was set to .01 because the *P* value for certain adjacent rows was as large as .002. The k-space rows identified in Table 1 were associated with movement because their timing coincided with visual observations of motion. Each movement was rapid and consequently affected only one or two k-space rows.

Images reconstructed from the k-space data between the rows identified in Table 1 showed the head and neck in different states of flexion (Fig 1). Images reconstructed from a small range of k_y values showed a ringing pattern, which was confirmed to be due to truncation artifacts when similar ringing was observed in images reconstructed from corresponding k-space segments acquired with the head stationary (17). Attempts to register the image from each segment with a reference image corresponding to k_y values from −10 cycles per FOV to 48 cycles per FOV yielded the displacement measurements in Table 1.

The uncertainty associated with displacement measurements was assessed by measuring displacements in images from specific k-space segments for which the displacement was known (Fig 2). Rotation was measured to within approximately 1°, even for large k_y values. Errors in measuring translation along the frequency-encoding direction (x) were between 1 and 2 pixels and were insensitive to the k_y about which the segment was centered. Errors in measuring translation along the phase-encoding direction (y) generally increased with k_y. When the experiment was repeated with segments consisting of 17 k_y values, rather than nine, the y-translation error encountered for the segment centered on the k_y value equal to 64 cycles per FOV was intermediate to

that for smaller and larger k_y values. Both the y-translation errors and their range for the different k_y values were smaller when the segments included a wider range of k_y values.

Ghostlike image artifacts and shading resulted from rotations applied directly to k-space (Fig 3). The ghost in the lower-left corner of Figure 3c, which typifies the other ghosts, had a mean intensity 60% that of the mean intensity in the midbrain on the reference image. This ratio decreased slightly to 50% when linear or cubic-spline interpolation was used (not shown). Rotation directly in k-space increased the midbrain intensity by as much as 55%, depending on the type of interpolation (Table 2). Also depending on the type of interpolation, regions farther from the center (eg, near the top of the head) became as much as 100 times less intense. Moreover, k-space rotations left gaps near the periphery of k-space. To confirm that these gaps were not responsible for the artifacts, an image was reconstructed from the central half of Figure 3d; this image resembled that in Figure 3c closely, although it had lower resolution. Spatial rotations left gaps in the corners of images, which were less noticeable because the corners were in the background. Measurements of the RMSE between the rotated images or k-space and the reference image or k-space (Fig 3a, 3b) are listed in Table 2. Smaller RMSE values were obtained for rotations in the spatial domain. Both the image and k-space RMSE values were smallest when cubic-spline interpolation was used in spatial-domain rotation.

Spatial transformations affecting only part of k-space caused image artifacts if the k-space was non-Hermitian (Fig 4). The artifacts causing blurring in Figure 4b can be traced to Figure 4a, which displays the phase after each row of the non-Hermitian rotation-corrected data was inverse Fourier transformed. The phase completed five cycles across each row in Figure 4a, because the echoes in the associated k-space peaked five columns before the center. The symmetry between the top and bottom halves of Figure 4c is missing in Figure 4a. Consequently, k-space was made as Hermitian as possible before spatial transformations affecting only part of a non-Hermitian k-space. This was accomplished through a spatial-domain phase correction derived from the largest central bipolar range of k_y values acquired with the head stationary (see Materials and Methods). The phase correction for the data acquired while the head moved was derived from the full range of k_x values and the k_y values between −10 and 10 cycles per FOV (Table 1).

The effect of erroneous displacement measurements on rotation and translation corrections depended on the central value of k_y in the k-space segment. The RMSE between several erroneously corrected images and the image of the stationary head is presented in Figure 5. Note that the RMSE varies with k_y similarly to the amplitude of k-space.

The k-space data acquired during motion were corrected as outlined in the Materials and Methods section with the measurements listed in Table 1 (Fig 6). Nearest-neighbor interpolation was used in correcting for rotation, although cubic-spline interpolation produced similar results. The uncorrected image (Fig 6a) had conspicuous ghosts and blurring and even showed different head positions. The correction reduced the ghosts and blurring, as shown in Figure 6d and Table 3. It was not informative to evaluate the correction by subtracting corrected images from Figure 6b, because of misregistration. No improvement in the image in Figure 6d was observed when

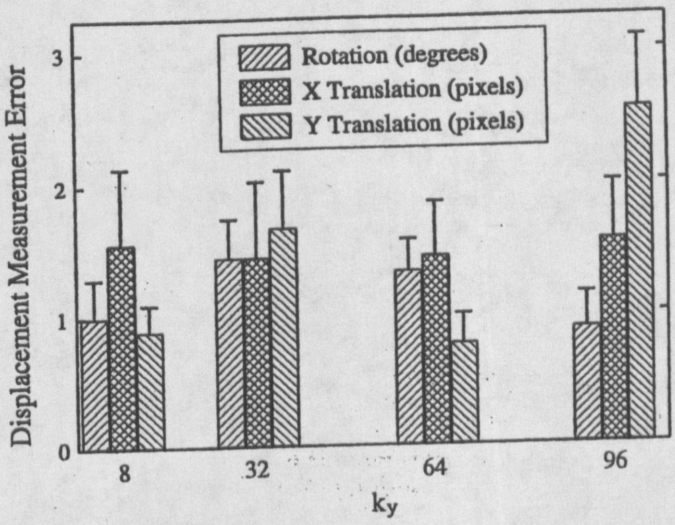

Figure 2. Errors in measurement of rotation and translation in images from k-space segments centered on different k_y values. Each segment consisted of 256 k_x values and nine k_y values. The mean errors from three individuals are shown, with the error bars representing the standard error of the mean.

Table 2
Comparison of Rotation in Space and K-space with Various Interpolation Methods

Domain	Interpolation	Figure 3	Midbrain Mean*	Top of Head Mean†	Image RMSE‡	K-space RMSE§	K-space Mean‖
K-space	Nearest-neighbor	c, d	155	1	37	109	71
K-space	Linear	NA	117	40	23	86	45
K-space	Cubic-spline	NA	115	46	21	90	41
Space	Nearest-neighbor	e, f	100	100	6	100	12
Space	Linear	NA	100	100	5	98	9
Space	Cubic-spline	g, h	100	100	4	99	8

Note.—NA = not available.
* Mean intensity in midbrain expressed as percentage of same region on reference image.
† Mean intensity near superior surface of brain expressed as percentage of same region on reference image.
‡ RMSE in entire difference image expressed as percentage of mean intensity in midbrain on reference image.
§ Mean modulus of entire k-space expressed as percentage of mean modulus of reference k-space.
‖ RMSE in entire k-space expressed as percentage of mean modulus of reference k-space.

the first and last row in each segment were corrected by using displacements intermediate to those for the neighboring segments. Comparison of Figure 6e with 6c and 6f with 6d reveals the improvement attributed to replacing rotation-corrupted data with unaffected data from the opposite side of k-space. Compared with Figure 6d, 6f was sharper and had less-intense ghosts.

• DISCUSSION

We confirmed the hypothesis that movement can be identified from its effects on k-space. The paired *t* test was effective for identifying k-space data acquired during subject movement. This identification was essentially automatic, and the *t* test threshold could have varied by one or two orders of magnitude without changing the results. However, further experience with this test is needed to evaluate its reliability for detecting k-space changes.

Features on images reconstructed from as few as nine k_y values were resolved well enough to allow accurate displacement measurements, although the accuracy was greater if the k-space segment included a wider range of k_y values or was centered on

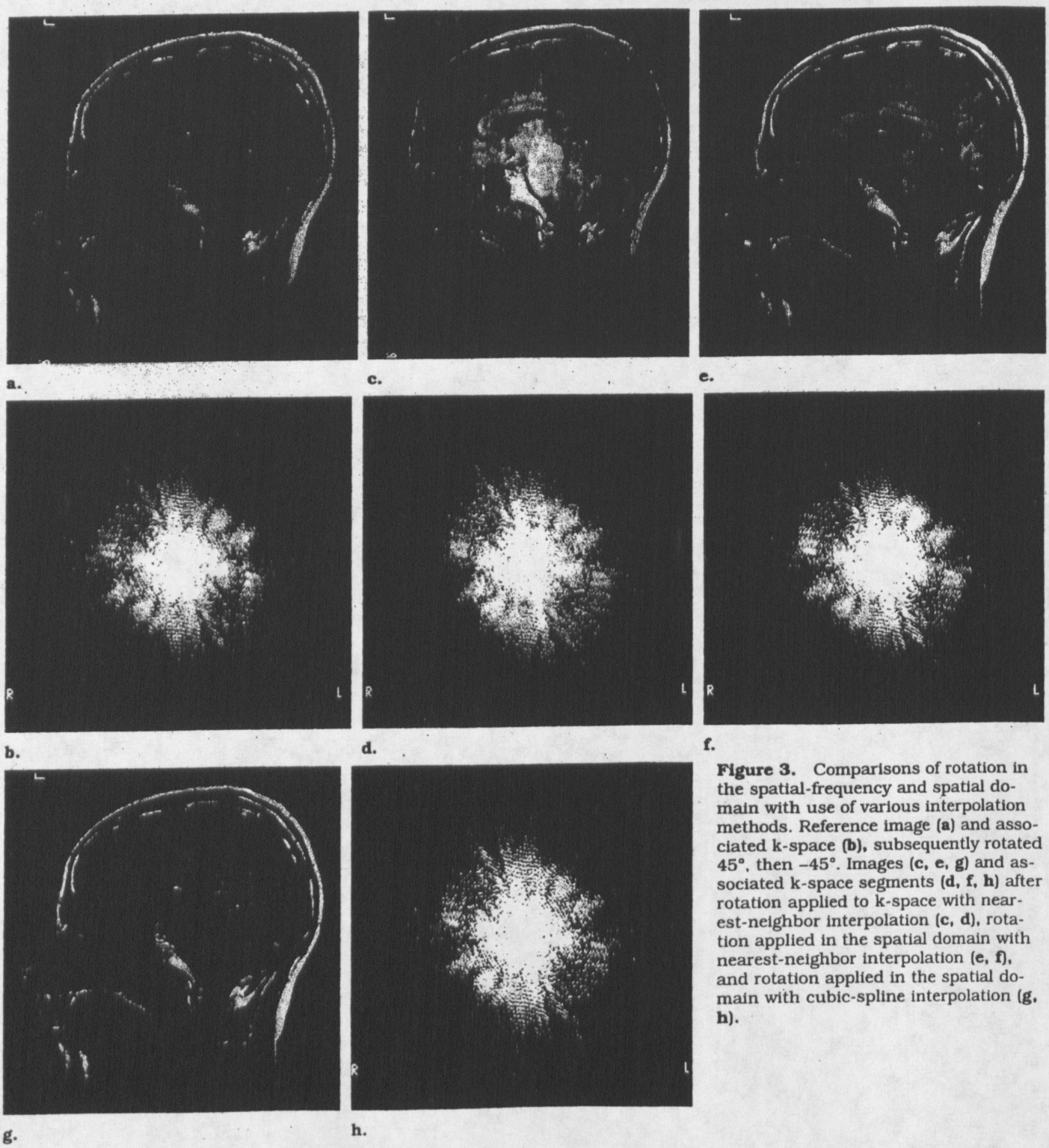

Figure 3. Comparisons of rotation in the spatial-frequency and spatial domain with use of various interpolation methods. Reference image **(a)** and associated k-space **(b)**, subsequently rotated 45°, then –45°. Images **(c, e, g)** and associated k-space segments **(d, f, h)** after rotation applied to k-space with nearest-neighbor interpolation **(c, d)**, rotation applied in the spatial domain with nearest-neighbor interpolation **(e, f)**, and rotation applied in the spatial domain with cubic-spline interpolation **(g, h)**.

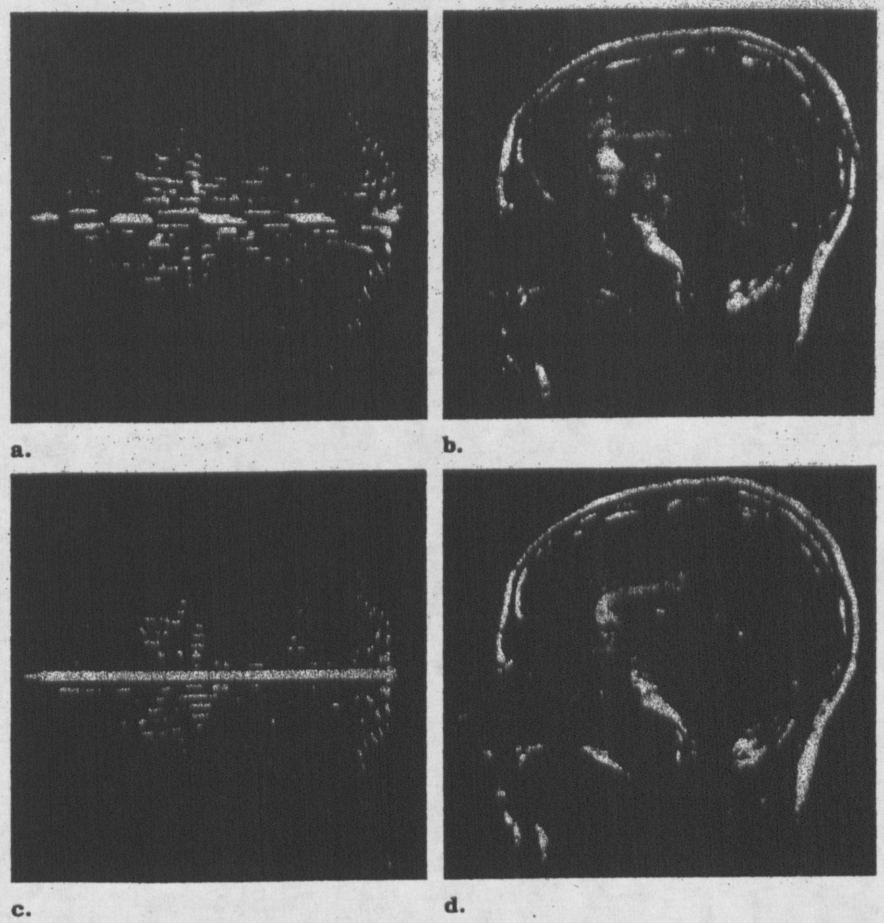

Figure 4. Demonstration of importance of making k-space Hermitian before compensating for rotation affecting a k-space segment. A rotation correction was applied to the first 126 rows ($-128 \leq k_y \leq -3$ cycles per FOV) of a non-Hermitian k-space (**a, b**) and a Hermitian k-space (**c, d**). (**a, c**) Phase of the complex numbers obtained after inverse Fourier transformation of each row of k-space and (**b, d**) modulus of the complex numbers obtained after a 2D inverse Fourier transformation of k-space. Note differences between the phase in the top and bottom halves of k-space in **a** and the associated blurring in **b**.

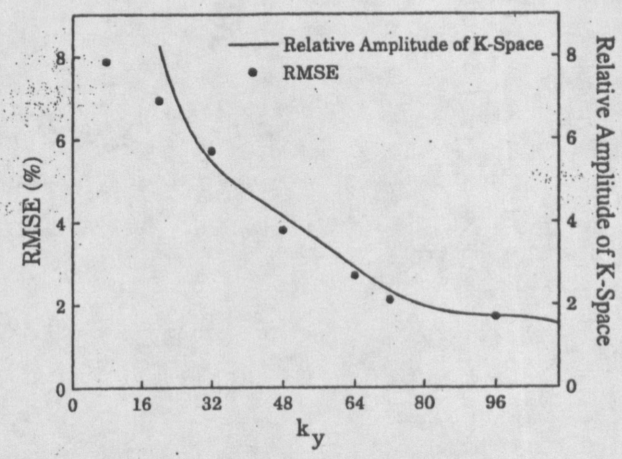

Figure 5. Influence of displacement-measurement errors on rotation and translation corrections. The displacement error was 2.0° and 2.0 pixels in both directions. Each segment spanned nine k_y values, with the central k_y value ranging from eight to 96 cycles per FOV. The RMSE between each erroneously corrected image and the image of the stationary head is presented. Superimposed on the RMSE is a plot representing the k_y dependence of the amplitude of k-space. The latter was calculated from a hybrid k-space formed by an inverse Fourier transform along k_x. The square root of the mean squared modulus of the central 100 pixels along x was calculated, and the results were normalized to the displacement-measurement error for k_y equal to 96 cycles per FOV.

a k_y value closer to zero. These displacement measurements might have been less accurate if ordered phase encoding or fast spin-echo sequences had been used, because the k_y values obtained with the head stationary would not have been contiguous and the k-space gaps would have caused truncation artifacts (18,19). Errors associated with translation along the x direction were largely insensitive to k_y, because each segment included the full range of k_x values. Perhaps the reason that rotation could be measured to within approximately 1° is that even a 1° rotation causes a two-pixel displacement at a location 114 pixels from the center of the FOV, and such a large displacement can be measured accurately. The method for measuring displacement could be refined to accommodate more general motion or reduce the need for human intervention (20–26). However, truncation artifacts and variable features on images from different k-space segments complicate automatic image registration.

Differences between rotations in the spatial domain and k-space, while not expected theoretically, should not be surprising. The image artifacts resulting from rotation in k-space are attributed to the interpolation, because the artifacts were nonexistent for 90° rotations, were less intense with smoother interpolation methods, and remained essentially unchanged when only the central half of k-space was used to form an image. Nearest-neighbor and cubic-spline interpolation were preferred over linear interpolation because they preserved the high spatial frequencies and minimized differences between the corrected and the reference k-spaces. If the objective had been to generate a smooth image, rather than to match the corrected k-space to the reference k-

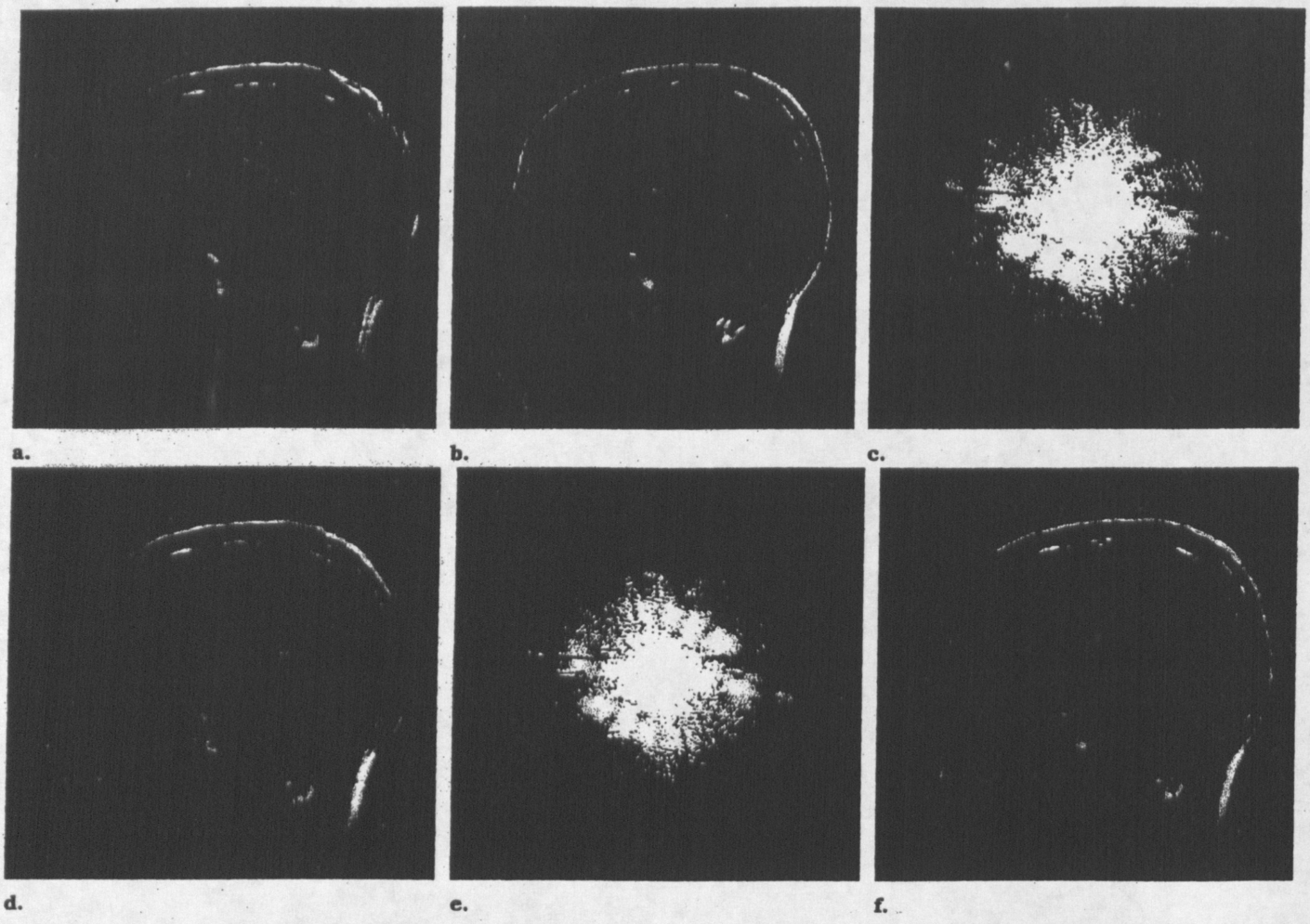

Figure 6. Planar-motion correction demonstrated on sagittal MR images of head of subject nodding sporadically. **(a)** Image degraded by motion; **(b)** reference image acquired with head stationary; **(c)** k-space and **(d)** image after correction, in which nearest-neighbor interpolation in the spatial domain was used for rotation; **(e)** k-space and **(f)** image after correction, followed by replacement of corrupted data with data corresponding to k_x and k_y of opposite sign, provided that these data had not also been corrupted by rotation.

Table 3
Effectiveness of Planar-Motion Correction

Figure 6	Image*	K-space†
a	91	46
b	5	0
c, d	37	43
e, f	37	39

* Mean modulus in 250-pixel background region near forehead.
† RMSE expressed as percentage of mean modulus of reference k-space.

space, cubic-spline interpolation would have been preferred, as in a related study (27).

Image artifacts resulting from a spatial transformation affecting only part of a non-Hermitian k-space arise because the pixels in MR images are represented by complex numbers. Rotation of the complex image associated with a non-Hermitian k-space alters the phase of each pixel, which causes artifacts by making the phase within each column or row inconsistent. The appearance of the artifacts depends on the number and location of the k_y values affected by the spatial transformation and the amplitude of the affected data relative to the rest of k-space. The proposed solution for making k-space closely Hermitian is feasible if there are enough data for the phase correction. Phase corrections based on k_y values between –8 and 8 cycles per FOV have been satisfactory for typical spin-echo images, although corrections for high-spatial-frequency phase variations benefit from a wider range of k_y values (15,16). The worst case would be movement during the acquisition of data indexed by k_y equal to ±1 cycle per FOV, for which only phase variations along the x direction could be corrected. Considering that motion affecting low-spatial-frequency data cause the most severe artifacts, such a partial phase correction might be acceptable.

The reduction of ghosts and blurring achieved in Figure 6d was good, considering that the image was acquired under realistic conditions and the correction did not require additional information, such as navigator echoes. The method assumed planar rigid-body motion. Although the motion seemed largely confined to the sagittal plane, there probably was some out-of-plane movement. Moreover, the corrections could not have been appropriate for k_y values acquired during movement, although special correc-

tions for these data showed no improvement. Perhaps intermediate corrections for the first and last rows of each k-space segment would have made a difference if the movements had lasted for more k_y values. Data at both ends of each segment were probably also degraded according to the speed and acceleration of the head, but these effects were not considered. Furthermore, the method assumes that the image retains the same intensity in different positions, which is a valid assumption to the extent that MR images are spatially invariant. Conditions that degrade the geometry or uniformity of MR images render the method less effective. Notable examples include magnetic field inhomogeneities with gradient-echo imaging techniques and nonuniform radio-frequency transmission or reception.

Comparison of Figure 6f with 6d reveals the extent to which data replacement reduced ghosts. The replacement procedure assumes a Hermitian k-space; otherwise, artifacts occur. For replacement to be effective, the corresponding data on the opposite side of k-space must have been acquired with the subject in the same position as for the reference k-space segment. This condition is not guaranteed. However, the reference segment generally has an asymmetric range of k_y, which allows replacement of some data in an adjacent segment.

In summary, a method for reducing the ghosts and blurring caused by planar motion has been developed. The timing and amount of displacement are measured from the k-space data without need for navigator echoes or external markers. The k-space is made as Hermitian as possible by a phase correction based on the largest symmetric range of k_x and k_y data acquired without displacement. Data from this closely Hermitian k-space acquired with the subject stationary are isolated and then copied to a blank array the same size as k-space. Hermitian symmetry is imposed on the array. A linear phase shift is then applied to correct for translation. Next, the array is inverse Fourier transformed into the spatial domain, rotated the desired amount with nearest-neighbor interpolation, and then Fourier transformed back to k-space. The corrected segment of data is copied to an array that becomes the corrected k-space. The procedure above is repeated for another k-space segment acquired in a different position. Data that are not to be corrected are copied to the corrected k-space last. To complete the correction, data corrupted by rotation are replaced by the complex conjugate of data corresponding to opposite-sign k_x and k_y, provided that the latter data were not also corrupted by rotation.

The method was tested specifically on rigid-body motion in 2D Fourier imaging, in which the phase-encoding gradient was incremented linearly. Usually, images of multiple sections are acquired together, in which case several images could be corrected on the basis of measurements from one image. The method could be adapted for more-general planar motion, general k-space trajectories, and three-dimensional imaging. Considering the promise shown by the basic method, these adaptations might be worthwhile subjects for future work.

Acknowledgments: The authors are grateful to Chris Macgowan and Ariff Kassam of the Department of Medical Biophysics, University of Toronto, and Cindy Stewart and David Mikulis, MD, of the Toronto Hospital for helping with the experiments.

References

1. Wood ML, Henkelman RM. MR image artifacts from periodic motion. Med Phys 1985; 12:143–151.
2. Haacke EM, Patrick JL. Reducing motion artifacts in two dimensional Fourier transform imaging. Magn Reson Imaging 1986; 4:359–376.
3. Wood ML, Xiang QS. Motion artifacts and remedies. In: Bronskill MJ, Sprawls P, eds. Medical physics monograph no. 21: the physics of MRI: 1992 AAPM Summer School Proceedings. New York, NY: American Institute of Physics, 1993; 383–411.
4. Wood ML, Ehman RL. Effects of motion in MR imaging. In: Stark DD, Bradley WG, eds. Magnetic resonance imaging. 2nd ed. St Louis, Mo: Mosby-Year Book, 1992; 145– 164.
5. Kumar A, Welti D, Ernst RR. NMR Fourier zeugmatography. J Magn Reson 1975; 18:69–83.
6. Twieg DB. The k-trajectory formulation of the NMR imaging process with applications in analysis and synthesis of imaging methods. Med Phys 1983; 10:610–621.
7. Xiang QS, Henkelman RM. K-space description for MR imaging of dynamic objects. Magn Reson Med 1993; 29:422–428.
8. Korin HW, Farzaneh F, Wright RC, Riederer SJ. Compensation for the effects of linear motion in MR imaging. Magn Reson Med 1989; 12:99–113.
9. Korin HW, Felmlee JP, Ehman RL, Riederer SJ, LaPlante CL. Adaptive corrections for rotational motion in MR imaging (abstr). In: Book of abstracts: Society of Magnetic Resonance in Medicine 1990. Berkeley, Calif: Society of Magnetic Resonance in Medicine, 1990; 560.
10. Ehman RL, Felmlee JP. Adaptive technique for high-definition MR imaging of moving structures. Radiology 1989; 173:255–263.
11. Felmlee JP, Ehman RI, Riederer SJ, Korin HW. Adaptive motion compensation in MR imaging without use of navigator echoes. Radiology 1991; 179:139–142.
12. Hedley M, Yan H. Motion artifact suppression: a review of post-processing techniques. Magn Reson Imaging 1992; 10:627–635.
13. Zang LH, Fielden J, Wilbrink J, Takane A, Koizumi H. Correction of translational motion artifacts in multi-slice spin-echo imaging using self calibration. Magn Reson Med 1993; 29:327–334.
14. Bracewell RN. The Fourier transform and its applications. 2nd ed. New York, NY: McGraw-Hill, 1978; 247.
15. Margosian P, Schmitt F, Purdy D. Faster MR imaging: imaging with half the data. Health Care Instrum 1986; 1:195–197.
16. MacFall JR, Pelc NJ, Vavrek RM. Correction of spatially dependent phase shifts for partial Fourier imaging. Magn Reson Imaging 1988; 6:143–155.
17. Wood ML, Henkelman RM. Truncation artifacts in MR imaging. Magn Reson Med 1985; 2:517–526.
18. Bailes DR, Gilderdale DJ, Bydder GM, et al. Respiratory ordering of phase encoding (ROPE): a method for reducing respiratory motion artifacts in MR imaging. J Comput Assist Tomogr 1985; 9:835–838.
19. Melki PS, Mulkern RV, Panych LP, Jolesz FA. Comparing the FAISE method with conventional dual-echo sequences. JMRI 1991; 1:319–326.
20. Pelizzari CA, Chen GTY, Spelbring DR, Weichselbaum RR, Chin C-T. Accurate three-dimensional registration of CT, PET, and/or MR images of the brain. J Comput Assist Tomogr 1989; 13:2–26.
21. Junck L, Moen JG, Hutchins GD, Brown MB, Kuhl DE. Correlation methods for the centering, rotation, and alignment of functional brain images. J Nucl Med 1990; 31:1220–1226.
22. Alpert NM, Bradshaw JF, Kennedy D, Correia JA. The principal axes transformation: a method for image registration. J Nucl Med 1990; 31:1717–1722.
23. Herbin M, Venot A, Devaux JY, et al. Automated registration of dissimilar images: application to medical imagery. Comput Vision Graphics Image Process 1989; 47:77–88.
24. Moshfeghi M. Elastic matching of multimodality medical images. Comput Vision Graphics Image Process 1991; 53:271–282.
25. Borgefors G. Hierarchical chamfer matching: a parametric edge matching algorithm. IEEE Trans Pattern Analysis Machine Intell 1988; 10:849–865.
26. Mandava VR, Fitzpatrick JM, Pickens DR III. Adaptive search space scaling in digital image registration. IEEE Trans Med Imaging 1989; 8:251–262.
27. Parker JA, Kenyon RV, Troxel DE. Comparison of interpolating methods for image resampling. IEEE Trans Med Imaging 1983; 2:31–39.

(48.) * Wood M., Shivji M., Stanchev P., "Planar-Motion Correction Using K-Space Data Acquired by Fourier MR Imaging", ***Journal of Magnetic Resonance Imaging,*** Vol. 5, 1994, 57-64.